Dr. D Powers

TPRD/B/0101/N82
WR/FBWG/P(82)68

Central Electricity Generating Board
Technology Planning and Research Division

Berkeley Nuclear Laboratories

Ref 6

PRE-TEST PREDICTION AND POST-TEST ANALYSIS OF PWR FUEL ROD BALLOONING IN THE MT-3 IN-PILE LOCA SIMULATION EXPERIMENT IN THE NRU REACTOR

By A.T. Donaldson, R.A. Horwood and T. Healey

June 1982

B-11
B-9

Printed By: Central Electricity Generating Board
Headquarters Services
Reprographic Section
Courtenay House
18 Warwick Lane
London EC4P 4EB
Telephone: 01-248 1202

Pre-Test Prediction and Post-Test Analysis of PWR
Fuel Rod Ballooning in the MT-3 In-Pile LOCA
Simulation Experiment in the NRU Reactor

- by -

A.T. Donaldson, R.A. Horwood and T. Healey

Approved

J. S. Waddington
23.6.82

Head of
Fuel and Component
Properties Section

For the attention of the Fuel Behaviour Working Group

SUMMARY

The USNRC and the UKAEA have jointly funded a series of in-pile LOCA simulation experiments in the Canadian NRU reactor in order to secure further information on the thermal hydraulic and clad deformation response of PWR fuel rod bundles. Test MT-3 in the series was performed using reflood rate and rod internal pressure conditions specified by the UK nuclear industry. The parameters were selected to ensure the development of a near-isothermal clad temperature history during which zircaloy was required to balloon and rupture near the alpha→alpha/beta phase transition. Specification of the reflood rate conditions was assisted by the performance of a precursor test on an unpressurised rod bundle and by complementary application of appropriate thermal hydraulic analyses. Identification of the rod internal pressure needed to cause ballooning and rupture was achieved using a creep deformation model, BALLOON, in conjunction with the clad thermal history defined by the prior thermal hydraulic test. This paper presents the basis of the BALLOON analysis and describes its application in calculating the fill gas pressure for rods MT-3, their axial ballooning profile and the clad temperature at peak radial strain elevations.

1. INTRODUCTION

The ballooning response of PWR fuel rods under postulated LOCA conditions has been the subject of intensive investigation during the past ten years. Experimental studies have included numerous out-of-pile and in-reactor tests on single rods and a smaller number of multi-rod experiments in out-of-pile facilities. To complement the latter work, a programme of in-reactor experiments on PWR fuel bundles was initiated by the Fuel Behaviour Research Branch of the United States Nuclear Regulatory Commission in conjunction with Pacific Northwest Laboratories. The major objectives of the project were to evaluate the thermal-hydraulic and mechanical deformation response of a full length PWR fuel bundle during the heat-up, reflood and quench phases of a LOCA. The facility selected for the test programme was the Canadian NRU reactor at Chalk River Nuclear Laboratory operated by the Atomic Energy of Canada.

The United Kingdom Atomic Energy Authority has contributed to the NRU programme on the basis that the UK industry would specify the test conditions for one of the experiments in the series. In particular, attention was focussed on the ballooning response of rods subjected to near-isothermal conditions for times between 100 and 200 seconds in the high alpha phase temperature range during reflood. To support the UK experiment, thermal-hydraulic analyses and clad creep deformation studies were undertaken. The former work indicated that the desired transient would be attained by varying the reflood rate and this was subsequently confirmed by precursor experiments on unpressurised fuel bundles in the NRU reactor.

To assist identification of the rod fill pressure needed to promote ballooning, mechanical property tests on NRU fuel cladding were also performed in conjunction with complementary creep modelling calculations. This paper summarises the work undertaken in support of the latter task, which has resulted in the development of a clad deformation model, BALLOON. Application of the model to assist evaluation of the fill gas pressure for the MT-3 rods is described and a comparison of the predicted and observed axial ballooning profiles is presented. It is shown that the average clad temperature of the peak ballooning regions can be evaluated from a knowledge of the measured clad temperature in the vicinity of peak strain regions, the rod pressure variation during ballooning and the steady state creep behaviour of zircaloy.

2. THE FUEL ROD DEFORMATION MODEL

2.1 Initial Geometry

The fuel rod configuration for the in-pile tests in the NRU reactor is illustrated in Figure 1. The model determines the axial ballooning profile of a 'nominal' fuel tube by sub-dividing it into 29 nodes each five inches long. Radial dilation of the nodes is unrestricted but no axial deformation is permitted; that is plane strain is assumed. Within each node, clad dilation is presumed to occur at constant metal volume and to remain uniform over the node length. Support grids are located at intervals along the length of the rods and are assumed to prevent local clad ballooning.

2.2 Input Parameters

The driving force for ballooning arises from the helium fill gas pressure in the fuel rods. In a closed system, the hot pressure of the fixed mass of gas varies as the tube expands and its internal volume increases. To predict the ballooning response of the cladding it is necessary to define;

(i) the initial tube length, diameter and wall thickness.

(ii) the initial total internal free volume of the fuel rod and its axial distribution.

(iii) the initial fill gas pressure at known volume and temperature.

(iv) the correlation between the instantaneous fill gas pressure and stress in the tube wall.

) the relationship between clad deformation rate and instantaneous stresses and temperature.

(vi) the thermal history of both the fill gas and the cladding.

The initial tube dimensions and the distribution of gas free volume in each of the 29 axial nodes are defined by the rod design parameters. These are summarised in Table 1. The initial fill gas pressure is a variable parameter and for the present study, calculations were performed using values equal to 450, 500 and 550 psi.

Tube ballooning was presumed to occur entirely by secondary creep in response to a hoop stress related to the instantaneous tube dimensions and internal pressure. The general creep equation for NRU zircaloy fuel cladding was determined in a parallel investigation[1]

The clad thermal history measured during a preceding thermal hydraulics test using unpressurised pins (TH - 2.14) was identified as a model transient

for the MT-3 ballooning experiment [2]. The thermocouple output from several rods at various axial levels, Figure 2, was used to construct a clad temperature profile for a 'nominal' rod undergoing the transient. The temperature-time-axial location array, interpolated from the thermocouple data, is shown in Table 2. The temperature-time history measured at axial levels 13 and 15 is compared for the TH2.14 test and the actual MT-3 experiment in Figures 3 and 4.

The filling gas temperature was presumed to be related to the instantaneous clad temperature. The effect on ballooning of gas temperatures equal to the instantaneous clad temperature T_c, and $T_c + 20^{\circ}$, 40° and 60°C respectively was examined.

2.3 Creep Deformation Analysis

Gas mass flow rates within the fuel tube assembly are assumed to be sufficiently rapid to maintain a homogeneous equilibrium pressure in the tube throughout a temperature transient. The pressure, P_E, in the fuel tube can therefore be calculated for any axial temperature profile and axial free volume distribution from the relation

$$\frac{P_o V_o}{T_o} = P_E \sum_{1}^{29} \left(\frac{V_i}{T_i}\right) \qquad (1)$$

where P_o is the cold fill pressure, V_o the total gas free volume at the filling temperature T_o; V_i and T_i are the free volume and mean gas temperature respectively in each axial node.

The clad axial temperature distribution varies with time during a transient and in the present calculation has been specified by the temperature-time-axial location array shown in Table 2.

The original gas free volume per axial node, $(V_i)_o$, is known, and the original tube internal volume per node, $(V_T)_o$, is given by the relation

$$(V_T)_o = \frac{\pi}{4} (d_o - 2t_o)^2 L_o \qquad (2)$$

where d_o, t_o and L_o are the tube outer diameter, wall thickness and node length respectively. The residual volume per node, V_K occupied by fuel, internal thermocouples and other instruments is given by difference as:

$$V_K = (V_T)_o - (V_i)_o \qquad (3)$$

This volume is assumed to remain invariant throughout the transient. It follows that the gas volume per node, $(V_i)_t$, at any time during the transient is

$$(V_i)_t = (V_T)_t - V_K \qquad (4)$$

where $(V_T)_t$ is the instantaneous tube volume per node, given by the relation

$$(V_T)_t = \frac{\pi}{4} (d_i - 2\, t_i)^2\, L_o \qquad (5)$$

The terms d_i and t_i are the instantaneous diameter and wall thickness and L_o is the unchanged node length.

Both d_i and t_i can be expressed in terms of the original tube dimensions, and the mid-wall diametral engineering strain, e, by the relations

$$\begin{aligned} d_i &= (d_o - t_o)\,(1 + e) + t_o\,(1 + e)^{-1} \\ t_i &= t_o\,(1 + e)^{-1} \end{aligned} \qquad (6)$$

Furthermore, the engineering strain, e, and true strain, ε, are related according to the expression

$$\varepsilon = \ell n\,(1 + e) \qquad (7)$$

whilst the true strain $(\varepsilon)_i$ in a given node at any time, t, during a transient is given by the integral

$$(\varepsilon)_i = \int_o^t \dot{\varepsilon}_i\, dt \qquad (8)$$

where $\dot{\varepsilon}_i$ is the instantaneous hoop strain rate and depends on the hoop stress, σ and the temperature T according to the expression [2]

$$\dot{\varepsilon}_i = A\,(\frac{G}{T})\,(\frac{\sigma}{G})^n \exp - \frac{Q_\ell}{RT} \qquad (9)$$

For the zircaloy-4 cladding used in the present series of NRU tests,

the structure constant $A = 6.54 \times 10^{16}\ N^{-1}\ m^2\ K\ sec^{-1}$

the stress exponent $n = 4.94 \pm 0.09$

and the temperature coefficient $Q_\ell = 294.0 \pm 16.0$ kJ $mole^{-1}$

The elastic shear modulus G ($N\ m^{-2}$) is given by

$$G = 3.326 \times 10^{10} - 2.244 \times 10^{7} (T - 273) + 2.161 \times 10^{3} (T - 273)^{2}$$

and RT has its usual meaning.

The integral in equation 8 may be solved by numerical iteration using the expressions

$$(\varepsilon)_i = \Sigma \Delta\varepsilon_i \qquad (10)$$

and $$\Delta\varepsilon_i = \dot{\varepsilon}_i \,\Delta t \qquad (11)$$

providing the time step, Δt, is sufficiently small for the strain rate, $\dot{\varepsilon}_i$, to be assumed to remain constant during the interval. Equation 9 may then be used to determine the appropriate strain rate, $\dot{\varepsilon}_i$, since the variation of temperature, T_i, with time is known, Table 2. The hoop stress, σ_i in a given node may be calculated from the expression

$$\sigma_i = \frac{P_E\ (d_i - t_i)}{2\ t_i} \qquad (12)$$

where P_E is the current equilibrium gas pressure and is determined by equation 1.

The preceding deformation analysis which forms the basis of the BALLOON model commences by calculating the equilibrium pressure at the start of the transient for the specified initial temperature profile and initial gas volume distribution. The initial hoop stress in each of the axial nodes along the fuel rod is evaluated using the initial rod dimensions. Initial strain rate and strain increment are calculated and the new tube volume after the first time step is recalculated together with the new gas volume. The new temperature profile is then imposed and a new equilibrium pressure is calculated. The iteration loop is repeated to determine the stress for the new node dimensions, and hence the new strain rate, strain, tube dimensions and gas volume. The entire calculation is repeated until the node with the largest strain has doubled its initial diameter when rupture is deemed to occur. Since the strain at which the iterative calculation stops is an input parameter, the model cannot predict a rupture strain. However once the tube strain

exceeds 0.3, the instantaneous strain rate is both large and accelerating. Consequently the model does yield a reasonable estimate of the time to rupture irrespective of the precise rupture criterion chosen.

4. PREDICTED BALLOONING RESPONSE AND ROD PRESSURE SELECTION

4.1 Near-Isothermal Conditions

The preceding model was used to evaluate the ballooning response of the 'nominal' rod in the MT-3 bundle when subjected to the thermal transient described in Table 2. The analysis was performed to establish the effect of rod fill gas pressures equal to 450, 500 and 550 psi on the axial ballooning profile and time-to-rupture. The predicted variation of maximum tube diameter and hot gas pressure as a function of the cold fill pressure for the clad thermal history described in Table 2 is shown in Table 3 and Figures 5a - c. As the initial cold fill pressure was increased from 450 to 550 psi, the calculated time to rupture decreased from a value in excess of 170 seconds to less than 100 seconds depending on the assumed hot gas temperature.

The calculated axial ballooning profiles are shown in Figures 6 to 8 for assumed gas temperatures equal to the clad temperature T_c, and in excess of T_c by 60^oC. Cold fill pressures of 450, 500 and 550 psi were again selected and comparison of the Figures shows that ballooning was predicted to occur over three grid spans for each pressure history. In all cases, the maximum radial strain was located at level 15 (node 20 - 21) whilst smaller strain peaks occurred at levels 13 and 17 corresponding to nodes 16 and 24.

4.2 Adiabatic Heating

The model was also used to examine the effect on rupture temperature of maintaining a clad thermal ramp of $8^oC\ sec^{-1}$ which corresponded to the adiabatic heating rate prior to reflood. For this calculation, it was assumed that the cladding experienced an axial thermal history identical

to that defined in Table 2 for the period up to 40 seconds. Temperatures at levels 13 to 17 (nodes 16 to 24) were then allowed to rise at $8^{o}C\ sec^{-1}$ (see Figures 3 and 4) whilst the remaining nodes maintained the temperature history specified in Table 2. Clad failure was predicted to occur appreciably earlier but at a higher temperature than calculated for the transient conditions defined by Table 2. Thus, for example, for a cold fill pressure of 550 psi and a clad-to-gas temperature difference of $60^{o}C$, the calculated rupture time was 51 seconds which

corresponded to a rupture temperature of $860^{o}C$. By contrast, rupture occurred at $t_r \sim 100$ seconds for the corresponding near isothermal transient. The small margin of 11 seconds between the occurrence of rupture during uncontrolled adiabatic heating and the required temperature turn-round time of 40 seconds to near-isothermal heating emphasised the need for precise control of the reflood rate parameters in the ' test.

4.3 R ressure Selection

An essential requirement of the MT-3 test was that rod-to-rod interaction should occur during the reflood phase of a near-isothermal transient lasting 100 to 200 seconds. On the basis of the above calculations, a cold fill pressure of 550 psi was selected for each of the twelve MT-3 rods. For a clad thermal transient identical to that defined by the precursor thermal hydraulic experiment, this pressure was predicted to promote ballooning strains in excess of 0.1 and 0.3 above level 13 and 15 respectively after approximately 100 seconds. Application of the lower pressure of 450 psi was predicted to require near isothermal heating in excess of 170 seconds to promote ballooning and rupture. In order to ensure adequate deformation during the thermal transient, but to minimise the risk of premature failure during adiabatic heating, the reflood parameters were modified for MT-3 to ensure earlier turn-over of the initial heat-up rate. Subsequent performance of the MT-3 experiment demonstrated that the required thermal conditions were attained at levels 13 and 15, Figures 3 and 4.

5. DISCUSSION

5.1 Comparison of Model Predictions with Experiment

Application of the creep deformation model, BALLOON, to predict the rod fill pressure requirements for any ballooning experiment is dependent on the prior availability of information describing the axial temperature history of the cladding. Such data were provided by the precursor thermal hydraulic experiment on an identical fuel bundle containing unpressurised rods. The introduction of fill gas pressures between 450 and 550 psi into rods sustaining such a transient was calculated to promote rod ballooning for which the predicted axial profiles are shown in Figures 6 to 8. Comparison of the predicted profiles with the typical measured ballooning response of rods in the MT-3 test, Figure 9, illustrates that there is good agreement in three important respects. First, the calculated response was characterised by the development of three strain peaks occupying adjacent intergrid spans in the vicinity of levels 13, 15 and 17. This is consistent with the observed profiles in the MT-3 test. Second, tube rupture was observed to occur towards the top of the intergrid span above level 15 at a height of 105 inches; the calculated location of the rupture zone was 100 inches. Finally, the observed mean strains at the peak deformation zones above levels 13 and 17 were respectively 0.13 and 0.02. These values are consistent with the model predictions of 0.11 and 0.01 respectively.

The levels of agreement between prediction and observation lends confidence to the use of the creep deformation model as an analysis tool for further calculations of the ballooning response of MT-3 rods. Thus, one rod (2C), containing thermocouples at levels 13 and 15 was also attached to a transducer which recorded the rod internal pressure variation up to rupture[3] Since the pressure history was defined, deformation of a single axial position could be examined in isolation provided its thermal history was known. For rod 2C, the measured pressure history, Figure 10, may be used in conjunction with the equations 8 to 12 to calculate the diametral strains at levels 13 and 15 for their respective temperature histories. Such a calculation

predicts large strains at level 13 and rupture at level 15 within 114 seconds. In fact, rod 2C did not rupture until ~ 122 seconds into the reflood transient. However, the pressure transducer on the same rod indicated an internal pressure of ~ 150 psi after rupture although the containment pressure was ~ 40 psi, Figure 10. It was assumed that this difference corresponded to a fixed zero error, ΔP, which persisted throughout the MT-3 transient. On this basis, the true internal pressure, P_{TRUE}, was related to the observed pressure, P_{OBS}, according to:

$$P_{TRUE} = P_{OBS} - \Delta P$$

The effect of transducer zero errors, in the range $100 \leq \Delta P \leq 200$ psi, on the strains predicted at levels 13 and 15 after 122 seconds was examined. A value of ΔP equal to 150 psi enabled the best agreement with the observed strains to be obtained and was in reasonable accord with the measured transducer zero error.

Clad temperature thermocouples were not located on the peak radial strain regions in rod 2C corresponding to axial elevations of 84 and 103 inches. However, by assuming that the temperature at each of the peak strain regions above nearby levels 13 and 15 was enhanced by constant but different values K_{84} and K_{103} throughout the transient according to

$$T_{103} = T_{97} + K_{103}$$

and

$$T_{84} = T_{76} + K_{84}$$

it was possible to perform strain calculations with ΔP equal to 150 for various values of K_{103} and K_{84} until $\varepsilon_{103}/\varepsilon_{97}$ and $\varepsilon_{84}/\varepsilon_{76}$ matched those observed in MT-3. On this basis, the temperature at the peak strain position (103 inches) exceeded that measured at level 15 (97 inches) by 16°C whilst the temperature calculated at the 84 inch elevation exceeded the measured value at level 13 (76 inches) by 54°C. The larger temperature difference required to match the respective strains at the lower axial positions possibly reflects the close proximity of the rising quench front to these locations during the latter stages of the MT-3 transient.

7. CONCLUSIONS

7.1 The deformation model, BALLOON, correctly predicts the occurrence of three axial strain peaks in the MT-3 rods. The calculated position of rupture and the relative peak strain heights are also in good agreement with observations.

7.2 The predicted rupture time depends on the initial fill gas pressure and on the relation assumed between the gas and clad temperatures. The range of rupture times ($100 \leq t_r \leq 170$ seconds) determined from the calculations brackets the experimental values.

7.3 The close agreement between model prediction and experiment lends confidence to the use of the creep model for additional analysis on instrumented fuel rods. In this respect radial strain matching between level 13 (76 inches) and the adjacent peak strain position for rod 2C (84 inches) requires a temperature enhancement of 54^{o}C. At the higher level of 103 inches, development of the observed strain profile requires the maintenance of a temperature differential of 16^{o}C above that experienced at 97 inches.

REFERENCES

[1] Donaldson, A.T., Horwood, R.A. and Healey, T. Central Electricity Generating Board Report TPRD/B/0007/N82 and "Water Reactor Fuel Element Performance Modelling", Preston, England, March 1982.

[2] Mohr, C. "Thermal Hydraulic Test No. 2 LOCA Simulation in NRU Reactor", NUREG/CR/2526 and Pacific Northwest Laboratory Report PNL 4164.

[3] Mohr, C. "Materials Test No. 3 LOCA Simulation in the NRU Reactor", NUREG/CR/2528 and Pacific Northwest Laboratory Report PNL 4166.

TABLE 1 : NRU Fuel Rod Internal Gas Volume and Tube Dimensions

Axial Nodes	Gas Volume per Node (cm^3)
1 → 3	0.65
4	0.58
5 → 13	0.30
14	0.33
15 → 22	0.39
23 → 27	0.48
28	1.53
29	7.82
	Total 20.43

Tube Outside Diameter 9.65 mm

Tube Wall Thickness 0.58 mm

TABLE 2

Axial Variation of Clad Temperature as a Function of Time into Transient

Node / Time	P-1	P-2	P-3	P-4	P-5	P-6	P-7	P-8	P-9	P-10	P-11	P-12	P-13	P-14	P-15	P-16	P-17	P-18	P-19	P-20	P-21	P-22	P-23	P-24	P-25	P-26	P-27	P-28	P-29
	Temperature, K																												
12s	450	450	450	487	524	561	598	635	672	674	674	698	748	760	771	783	792	802	811	821	815	808	802	796	778	759	741	723	659
14s	449	449	449	489	528	568	607	647	686	694	694	719	769	780	792	803	812	821	830	838	831	823	816	808	788	768	748	728	659
16s	449	449	449	491	532	574	616	658	700	709	709	736	790	801	811	822	831	839	848	856	847	838	830	821	799	777	755	734	659
18s	449	449	449	493	537	581	626	670	714	724	724	752	810	820	831	842	850	858	866	875	864	854	843	833	809	786	762	739	659
20s	401	401	401	455	509	563	618	672	726	733	733	765	829	840	850	860	868	876	884	892	880	869	857	845	820	795	770	744	659
22s	403	403	403	458	512	566	621	675	729	727	727	766	845	856	867	879	886	894	901	909	896	883	871	858	831	804	778	751	660
24s	391	391	391	450	509	568	627	686	746	729	729	774	863	874	885	896	904	911	919	926	912	898	885	871	842	814	785	757	663
26s	383	383	383	444	505	567	628	689	751	707	707	764	878	890	902	914	921	928	936	943	928	913	898	883	853	824	794	764	668
28s	383	383	383	444	505	567	628	689	751	685	685	752	887	901	916	930	937	945	952	959	943	928	912	896	865	834	802	771	674
30s	378	378	378	438	498	558	619	679	739	602	602	699	893	910	928	945	952	960	967	974	958	941	925	908	875	843	811	778	682
32s	377	377	377	439	501	563	625	687	750	611	611	709	903	922	941	959	967	974	982	989	971	954	936	919	885	851	818	784	690
34s	377	377	377	441	505	569	633	698	762	411	411	578	912	931	950	969	976	983	990	998	980	962	944	926	891	856	820	785	696
36s	371	371	371	436	500	565	629	694	758	406	406	576	917	938	960	981	988	995	1002	1009	990	971	953	934	897	861	824	788	698
38s	366	366	366	429	492	555	618	681	744	406	406	580	928	949	970	991	998	1004	1011	1018	998	978	959	939	902	864	827	790	698
40s	359	359	359	416	473	529	586	643	700	407	407	576	914	942	970	998	1004	1011	1017	1023	1004	984	964	944	905	866	827	789	694
42s	362	362	362	422	482	542	602	662	723	407	407	579	923	950	977	1004	1010	1016	1022	1028	1007	986	965	944	904	864	825	785	685
44s	357	357	357	414	472	529	586	644	701	408	408	580	923	952	981	1010	1016	1021	1027	1032	1011	989	968	946	905	864	824	783	676
46s	350	350	350	359	369	378	388	397	407	407	407	575	911	946	981	1016	1022	1027	1032	1037	1015	992	970	947	906	865	824	783	665
48s	350	350	350	359	369	378	388	397	407	406	406	578	922	954	987	1019	1024	1029	1033	1038	1016	993	971	948	906	863	820	777	654
50s	350	350	350	359	369	378	387	396	406	404	404	582	937	966	995	1024	1028	1033	1037	1041	1018	994	971	948	904	860	816	773	642
52s	346	346	346	356	366	376	386	396	406	404	404	574	912	951	989	1028	1032	1036	1041	1045	1021	997	973	949	904	860	815	771	631
54s	345	345	345	355	364	374	384	393	403	404	404	575	918	954	991	1028	1032	1037	1041	1046	1022	998	974	950	904	858	812	766	621
56s	346	346	346	356	366	375	385	395	404	404	404	578	927	961	996	1031	1035	1039	1043	1048	1023	999	974	950	903	856	809	762	607
58s	346	346	346	355	365	374	384	394	403	403	403	578	929	964	999	034	1038	1041	1045	1048	1024	999	974	950	9C1	853	805	757	579
60s	345	345	345	354	364	373	383	392	402	404	404	573	912	952	993	1033	1037	1041	1044	1048	1024	999	974	950	900	851	801	752	538
62s	346	346	346	355	365	374	384	394	403	403	403	573	913	954	996	038	1041	1044	1047	1050	1025	1000	975	950	900	850	800	750	503
64s	344	344	344	354	364	373	383	393	403	403	403	569	902	949	995	1042	1044	1047	1050	1053	1028	1002	977	952	901	850	799	748	483
66s	344	344	344	354	363	372	381	391	400	403	403	567	896	945	995	1045	1047	1049	1052	1054	1029	1003	978	952	901	849	797	745	467
68s	344	344	344	354	363	373	383	392	402	403	403	567	896	947	997	1048	1050	1052	1054	1055	1030	1004	978	952	900	848	795	743	456
70s	343	343	343	352	362	371	380	389	399	404	404	561	876	934	991	1049	1051	1053	1055	1057	1031	1005	979	954	900	847	794	740	449
72s	342	342	342	351	360	369	377	386	395	403	403	555	860	924	987	1051	1052	1054	1056	1058	1032	1006	980	954	900	846	792	738	444
74s	342	342	342	352	361	371	380	390	399	404	404	554	853	920	987	1054	1055	1056	1058	1059	1033	1007	981	955	901	846	791	736	441
76s	343	343	343	353	363	373	383	393	403	404	404	551	844	915	986	1058	1059	1060	1061	1062	1035	1009	983	956	901	846	791	736	438
78s	342	342	342	352	361	371	380	390	399	403	403	546	834	910	986	1062	1063	1064	1065	1065	1039	1012	986	959	904	848	793	737	439
80s	340	340	340	350	360	370	379	389	399	404	404	540	812	896	980	1065	1066	1067	1068	1069	1043	1016	990	963	907	851	795	739	443
82s	340	340	340	350	359	369	379	388	398	403	403	534	797	886	975	1065	1066	1068	1070	1071	1045	1018	992	966	909	853	797	740	447
84s	340	340	340	350	359	368	377	386	395	402	402	528	779	875	970	1065	1068	1070	1072	1074	1048	1021	995	969	912	856	800	743	450
86s	340	340	340	349	359	368	377	387	396	403	403	525	770	870	971	1071	1073	1075	1077	1078	1052	1026	999	973	916	860	804	747	455
88s	340	340	340	350	360	370	380	390	399	404	404	403	403	626	850	1074	1076	1078	1080	1083	1056	1029	1003	976	920	863	807	751	461
90s	340	340	340	351	361	371	381	391	401	404	404	404	403	628	852	1077	1079	1082	1084	1086	1060	1033	1007	980	924	867	811	755	469
92s	342	342	342	352	363	373	383	394	404	404	404	404	403	627	851	1075	1079	1082	1085	1089	1062	1036	1010	984	927	870	813	756	475
94s	342	342	342	353	363	373	384	394	404	404	404	404	403	627	852	1076	1080	1083	1087	1090	1064	1038	1012	986	929	872	815	758	480
96s	342	342	342	353	363	373	384	394	404	404	404	404	404	628	852	1076	1080	1084	1088	1092	1066	1041	1015	989	932	874	817	760	483
98s	342	342	342	352	362	372	382	392	403	404	404	404	404	628	852	1076	1080	1084	1089	1093	1067	1042	1017	991	934	876	819	761	483
100s	342	342	342	352	361	371	380	389	399	406	406	405	404	628	851	1071	1080	1084	1089	1094	1069	1044	1019	994	936	878	820	762	481
102s	342	342	342	351	360	369	378	387	396	403	403	404	404	628	851	1074	1079	1085	1090	1095	1070	1045	1020	995	937	878	820	762	476
104s	342	342	342	351	359	367	375	384	392	399	399	401	405	627	850	1072	1078	1083	1089	1094	1070	1045	1020	995	936	878	820	762	470
106s	342	342	342	352	361	370	380	389	398	404	404	404	405	527	848	1070	1076	1082	1087	1093	1069	1044	1019	994	936	878	819	761	463
108s	343	343	343	351	360	368	376	385	393	403	403	404	405	624	844	1064	1070	1077	1084	1090	1066	1041	1017	992	934	875	816	758	455
110s	343	343	343	352	360	369	378	386	395	403	403	403	405	624	843	1062	1068	1075	1081	1088	1064	1040	1015	991	932	874	815	756	447
112s	343	343	343	352	360	369	377	386	394	405	405	405	405	622	839	1055	1063	1070	1077	1084	1061	1037	1013	990	930	870	810	751	442
114s	342	342	342	351	359	367	376	384	393	403	403	404	405	619	833	1046	1055	1064	1072	1081	1058	1035	1012	989	928	868	807	746	439
116s	340	340	340	349	357	365	373	381	389	391	391	395	404	617	829	1041	1051	1060	1070	1080	1057	1034	1011	988	927	865	803	742	437
118s	340	340	340	349	358	367	375	384	393	399	399	401	404	615	825	1036	1046	1056	1067	1077	1055	1032	1009	987	925	863	801	739	435
120s	340	340	340	349	357	366	375	384	393	401	401	402	404	612	821	1030	1041	1053	1064	1076	1053	1030	1007	984	922	860	798	736	433
122s	339	339	339	348	357	365	374	383	391	401	401	401	403	609	816	1022	1035	1048	1061	1074	1051	1029	1006	984	921	858	795	732	433
124s	339	339	339	348	357	366	375	384	393	402	402	402	403	607	811	1016	1030	1044	1059	1073	1051	1028	1006	984	920	857	794	731	432
126s	339	339	339	349	359	369	379	389	399	404	404	403	402	604	806	1008	1024	1040	1056	1072	1050	1028	1005	983	920	856	793	729	432
128s	339	339	339	349	359	369	379	389	399	403	403	403	403	601	800	998	1017	1035	1053	1071	1050	1028	1006	985	921	857	793	729	434
130s	339	339	339	348	358	367	377	386	396	403	403	403	403	598	794	990	1011	1032	1053	1074	1052	1031	1010	988	924	860	796	732	439
132s	337	337	337	346	355	365	374	383	393	403	403	403	403	599	794	990	1011	1033	1055	1077	1055	1034	1013	991	928	864	800	736	443
134s	337	337	337	348	358	369	380	390	401	404	404	404	403	597	791	986	1009	1033	1056	1080	1058	1037	1016	994	931	868	805	742	450
136s	338	338	338	349	360	371	382	393	404	404	404	404	404	595	786	977	1003	1029	1055	1081	1060	1039	1018	997	934	870	807	744	458
138s	339	339	339	350	360	371	382	393	404	404	404	404	404	591	778	965	994	1023	1052	1081	1061	1040	1020	999	936	873	810	747	464
140s	339	339	339	350	361	372	383	394	405	405	405	405	404	588	772	956	988	1020	1051	1083	1063	1043	1023	1003	940	876	813	750	469
142s	339	339	339	350	361	372	383	394	405	405	405	405	404	585	765	945	980	1014	1049	1084	1064	1044	1024	1004	941	878	815	752	471
144s	339	339	339	350	361	372	383	394	405	405	405	405	404	577	750	923	963	1004	1044	1084	1065	1045	1026	1007	943	880	817	754	474
146s	339	339	339	350	361	372	383	394	405	405	405	405	404	470	536	601	722	843	964	1085	1066	1047	1028	1009	945	882	818	755	475
148s	339	339	339	350	361	372	383	393	404	404	404	404	404	444	484	523	664	805	945	1086	1067	1048	1029	1011	947	884	820	757	475
150s	340	340	340	350	361	371	382	392	403	405	405	405	404	432	461	489	638	787	937	1086	1068	1050	1032	1014	950	886	822	759	477
152s	340	340	340	351	361	371	381	391	401	404	404	404	404	425	445	466	622	777	932	1087	1070	1052	1034	1016	953	889	825	762	480
154s	340	340	340	351	361	371	382	392	403	405	405	404	403	419	435	451	610	769	928	1087	1070	1053	1035	1018	955	891	827	764	485
156s	341	341	341	351	361	370	380	390	399	404	404	404	403	416	429	442	603	765	926	1088	1071	1055	1038	1021	957	894	830	766	490
158s	342	342	342	352	362	372	382	392	402	404	404	404	403	414	424	435	598	762	925	1089	1072	1056	1040	1024	961	897	834	770	497
160s	342	342	342	352	362	372	382	392	402	404	404	404	403	412	421	430	595	760	925	1090	1075	1059	1043	1028	964	901	838	774	504
162s	344	344	344	353	362	372	381	390	399	404	404	404	403	412	420	428	594	760	926	1092	1077	1062	1046	1031	968	905	842	779	513
164s	344	344	344	354	364	374	384	394	404	404	404	404	403	411	419	427	593	760	927	1094	1079	1064	1049	1035	972	909	846	783	522
166s	344	344	344	354	364	374	384	394	404	404	404	404	404	411	419	427	594	761	928	1095	1081	1067	1052	1038	975	912	849	786	531
168s	346	346	346	355	365	375	385	395	404	404	404	404	404	411	419	427	594	762	929	1097	1083	1069	1055	1041	979	916	854	791	538
170s	346	346	346	355	365	375	385	395	404	404	404	404	404	411	419	427	594	762	930	1097	1084	1071	1058	1045	983	921	859	797	547
172s	347	347	347	356	366	376	385	395	404	404	404	404	404	412	419	427	595	763	931	1099	1087	1074	1062	1049	987	926	864	802	556

NOTE : Temperature Values Interpolated from Experimental Data Determined in NRU Thermal Hydraulics Test TH2.14

TABLE 3

Variation of Maximum Tube Diameter and Hot Gas Pressure as a Function of Cold Fill Pressure and Time into Transient

	COLD FILL PRESSURE PO=3.1 MPa (450 psi)								COLD FILL PRESSURE PO=3.45 MPa (500 psi)								COLD FILL PRESSURE 3.79 MPa (550 psi)							
KO(C)	0		20		40		60		0		20		40		60		0		20		40		60	
Time into Transient secs	Dmax mm	Phot MPa	Dmax mm	Phot MPa	Dmax mm	Phot MPa	Dmax mm	Phot MPa	Dmax mm	Phot MPa	Dmax mm	Phot MPa	Dmax mm	Phot MPa	Dmax mm	Phot MPa	Dmax mm	Phot MPa	Dmax mm	Phot MPa	Dmax mm	Phot MPa	Dmax mm	Phot MPa
12	9.65	6.95	9.65	7.17	9.65	7.38	9.65	7.6	9.65	7.72	9.65	7.96	9.65	8.21	9.65	8.44	9.65	8.49	9.65	8.76	9.65	9.03	9.65	9.29
20	9.65	7.1	9.65	7.32	9.65	7.54	9.65	7.76	9.65	7.89	9.65	8.14	9.65	8.38	9.65	8.62	9.65	8.68	9.65	8.95	9.65	9.22	9.65	9.49
30	9.653	7.1	9.653	7.33	9.653	7.56	9.654	7.78	9.654	7.89	9.655	8.14	9.656	8.39	9.657	8.64	9.657	8.67	9.658	8.95	9.659	9.23	9.661	9.5
40	9.678	7.01	9.682	7.24	9.688	7.47	9.694	7.69	9.697	7.77	9.705	8.02	9.714	8.26	9.724	8.51	9.725	8.51	9.738	8.78	9.753	9.04	9.77	9.29
50	9.73	6.4	9.745	6.62	9.761	6.84	9.78	7.05	9.785	7.05	9.811	7.28	9.839	7.5	9.872	7.71	9.87	7.65	9.911	7.88	9.958	8.1	10.012	8.3
60	9.788	6.03	9.815	6.23	9.846	6.43	9.881	6.61	9.886	6.59	9.933	6.79	9.987	6.98	10.049	7.15	10.039	7.09	10.118	7.27	10.211	7.43	10.319	7.57
70	9.836	5.41	9.874	5.61	9.918	5.79	9.969	5.96	9.971	5.89	10.038	6.08	10.118	6.25	10.21	6.4	10.186	6.3	10.306	6.46	10.45	6.59	10.625	6.69
80	9.889	5.26	9.941	5.45	10.001	5.62	10.071	5.77	10.067	5.7	10.162	5.87	10.274	6.01	10.409	6.13	10.363	6.04	10.54	6.16	10.761	6.25	11.045	6.3
90	9.986	5.21	10.063	5.37	10.155	5.51	10.264	5.63	10.25	5.59	10.398	5.71	10.581	5.8	10.81	5.87	10.719	5.83	11.032	5.88	11.466	5.88	12.122	5.81
100	10.157	5.21	10.281	5.33	10.433	5.43	10.619	5.5	10.59	5.49	10.856	5.54	11.211	5.55	11.712	5.51	11.506	5.55	12.301	5.45	13.962	5.22	TR<	100
110	10.341	4.95	10.523	5.04	10.754	5.1	11.053	5.13	11.006	5.13	11.471	5.11	12.197	5.03	13.621	4.81	12.994	4.93	TR<	112	TR<	104	-	-
120	10.457	4.77	10.681	4.84	10.975	4.88	11.376	4.87	11.309	4.87	11.987	4.81	13.305	4.61	TR<	120	15.775	4.28	-	-	-	-	-	-
130	10.549	4.71	10.812	4.77	11.166	4.79	11.674	4.75	11.586	4.76	12.537	4.64	15.242	4.23	-	-	TR<	124	-	-	-	-	-	-
140	10.69	4.8	11.017	4.83	11.482	4.82	12.217	4.73	12.09	4.76	13.863	4.5	TR<	136	-	-	-	-	-	-	-	-	-	-
150	10.88	4.55	11.304	4.54	11.964	4.48	13.288	4.29	13.018	4.34	TR<	150	-	-	-	-	-	-	-	-	-	-	-	-
160	11.088	4.5	11.642	4.46	12.625	4.34	15.575	3.93	14.956	4.03	-	-	-	-	-	-	-	-	-	-	-	-	-	-
170	11.451	4.56	12.314	4.46	14.526	4.15	TR<	164	TR<	166	-	-	-	-	-	-	-	-	-	-	-	-	-	-
180	TR>	172	TR>	172	TR>	172	-	-	-	-	-	-	-	-	-	-	-	-	-	-	-	-	-	-

NOTE : a) KO = Temperature Difference Between Gas (TG) & Clad (TC)
b) Phot = Filling Gas Pressure at any Time During the Transient
c) Dmax = Maximum Tube Diameter at any Time During the Transient
d) Thermal History is as Shown in Table 1

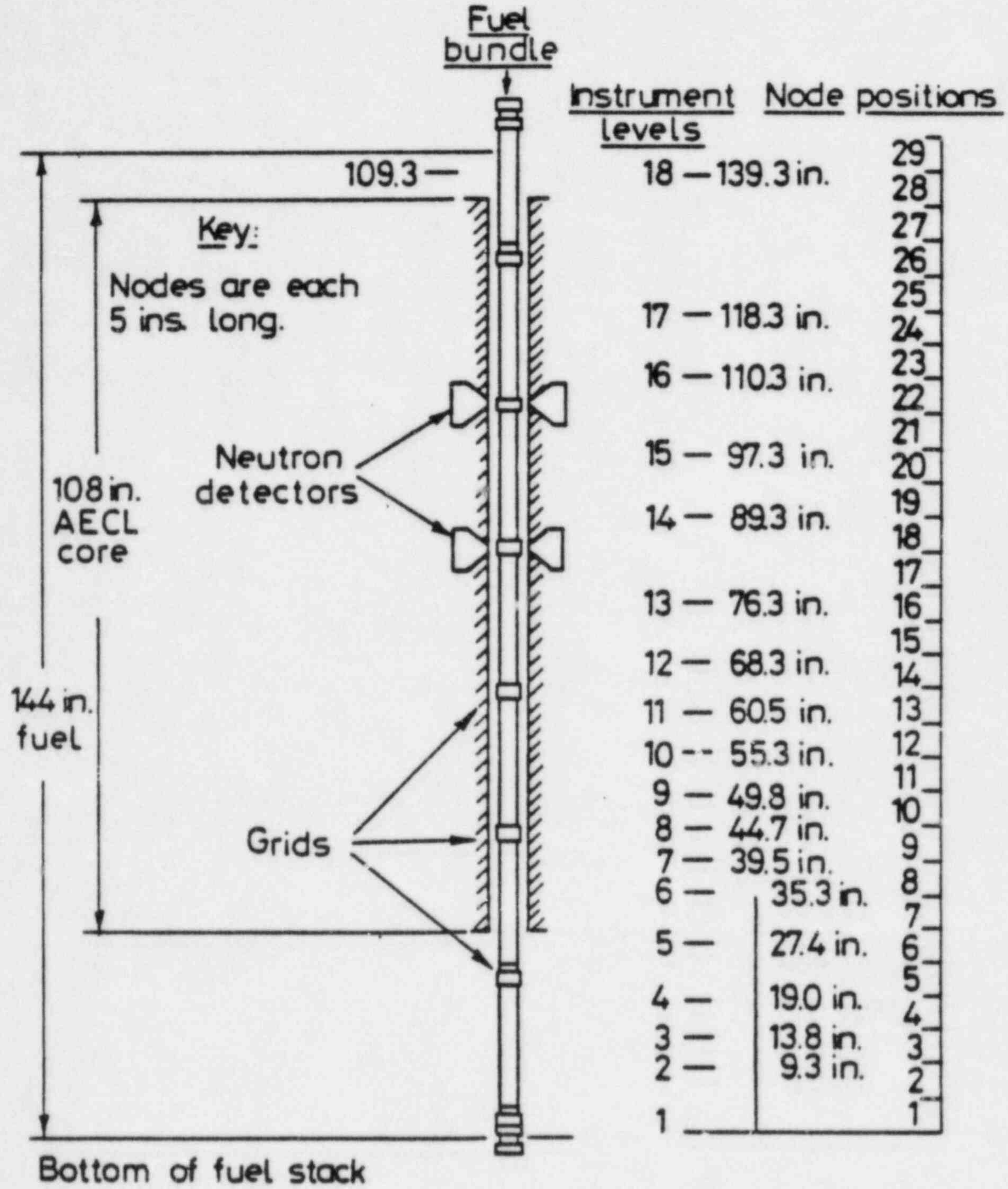

FIG. 1. Schematic Illustration of NRU Fuel Bundle Rods.

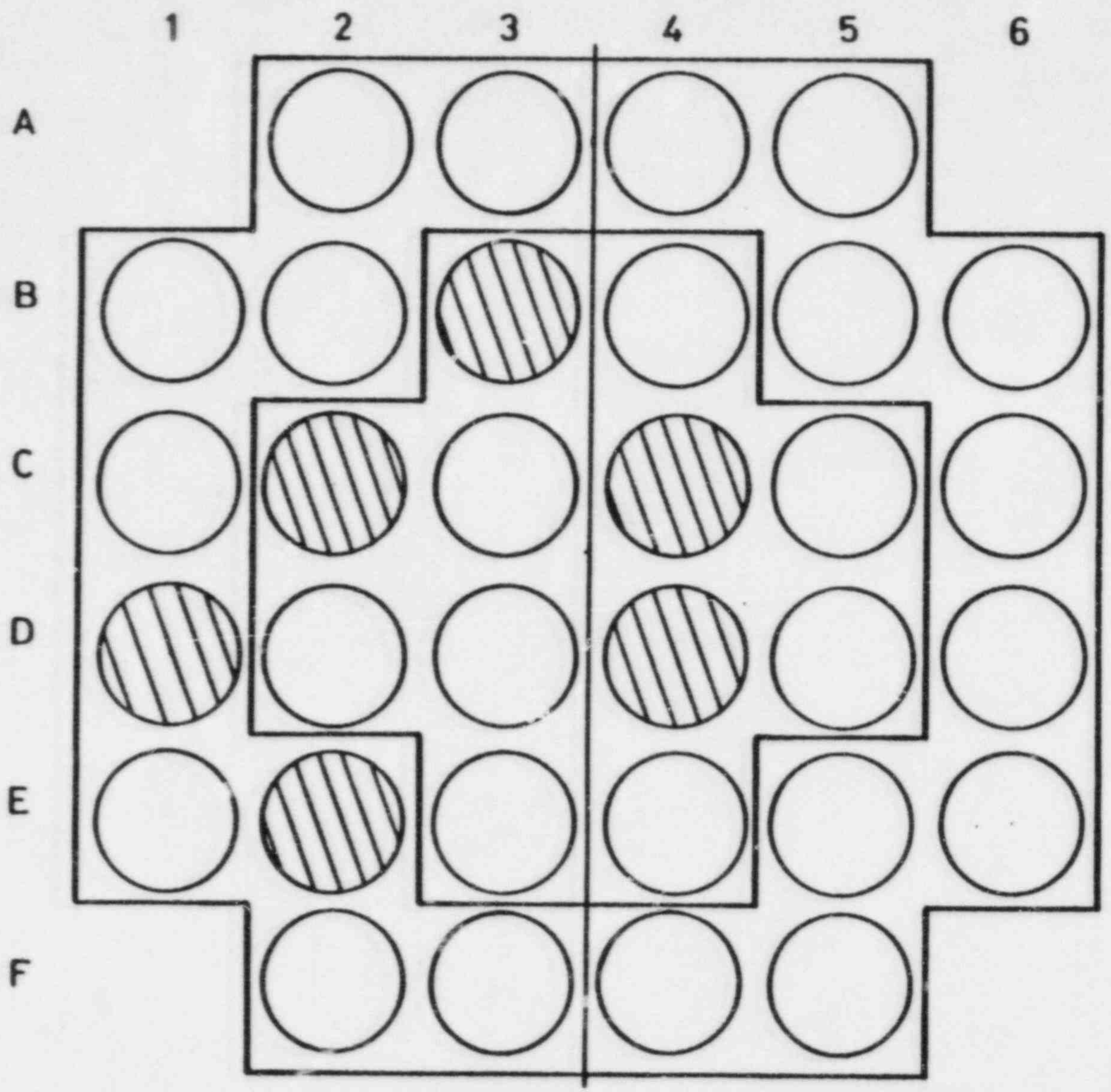

Rod number	Sensor ref. number	T/C level
2E	8	3
2E	24	8
2E	29	9
1D	39	11
3B	47	13
3B	61	15
4C	83	17
2C	115	18
4D	77	{ Plenum 19

FIG.2. Cross-Section of NRU Test Bundle; Thermocouples in Shaded Rods have been used to Construct an Axial Temperature Profile for Test TH-2.14.

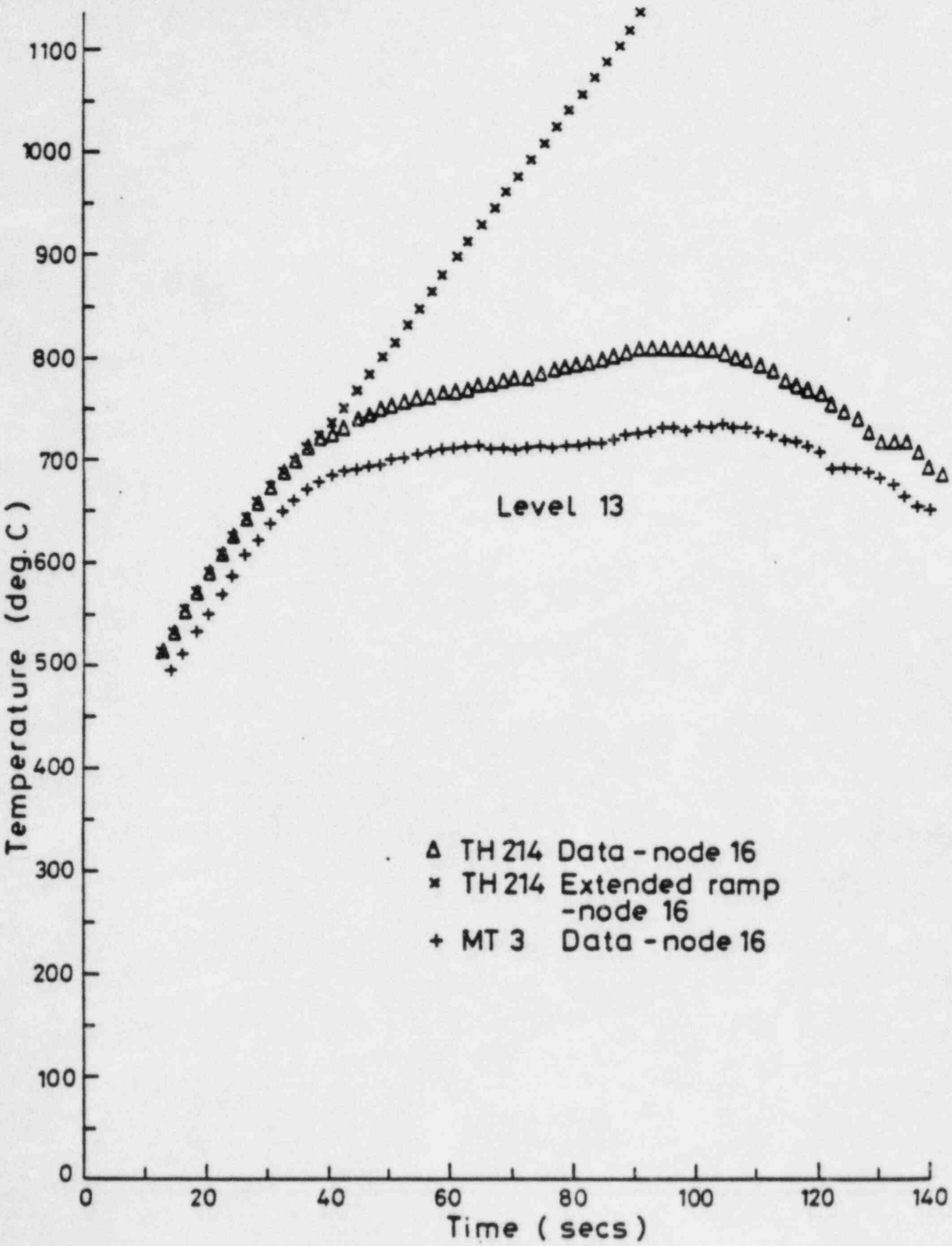

FIG.3. Temperature vs. Time Profiles at Axial Level 13 in Tests MT-3 & TH 2.14.

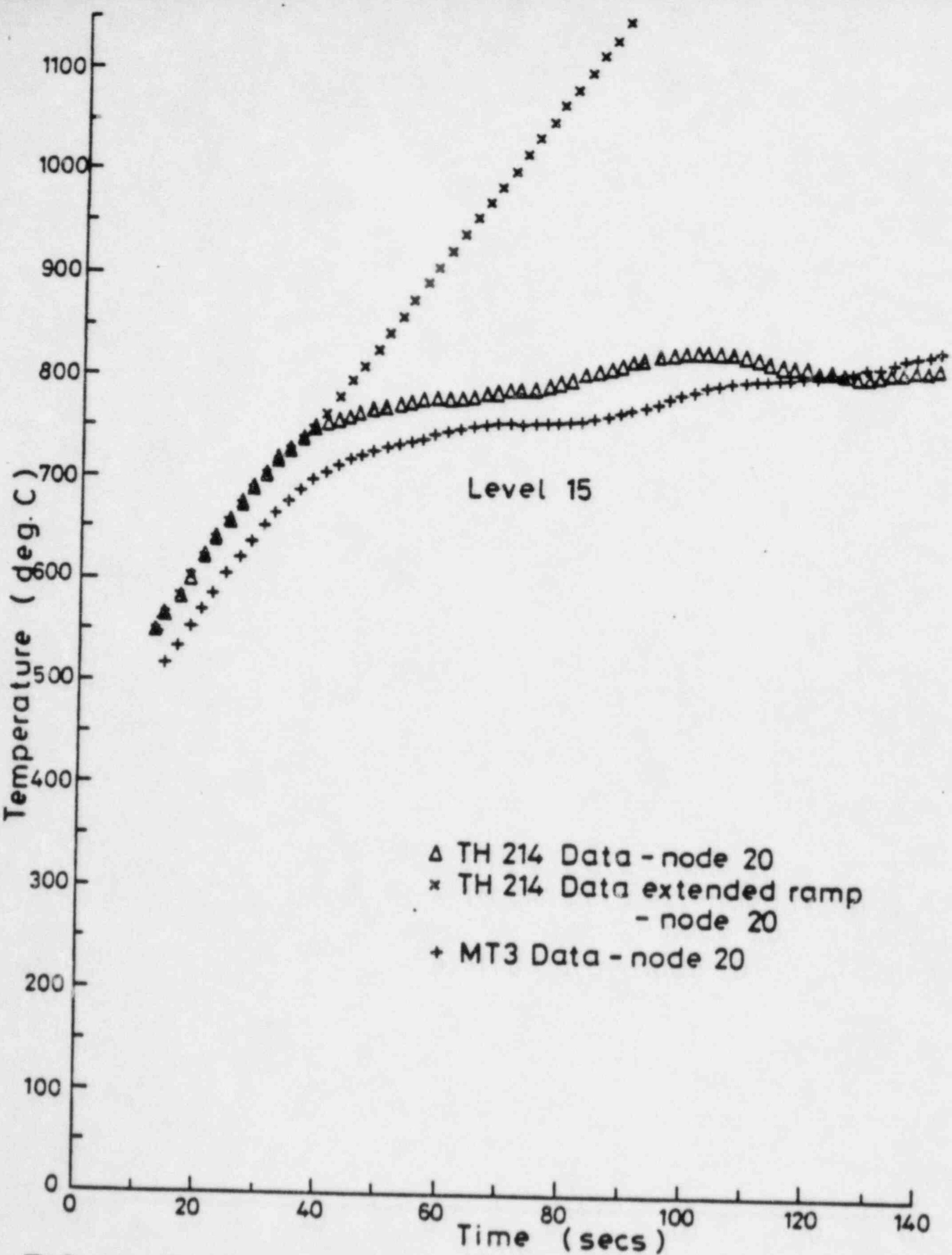

FIG. 4. Temperature vs. Time Profiles at Axial Level 15 in Tests MT-3 & TH-2.14.

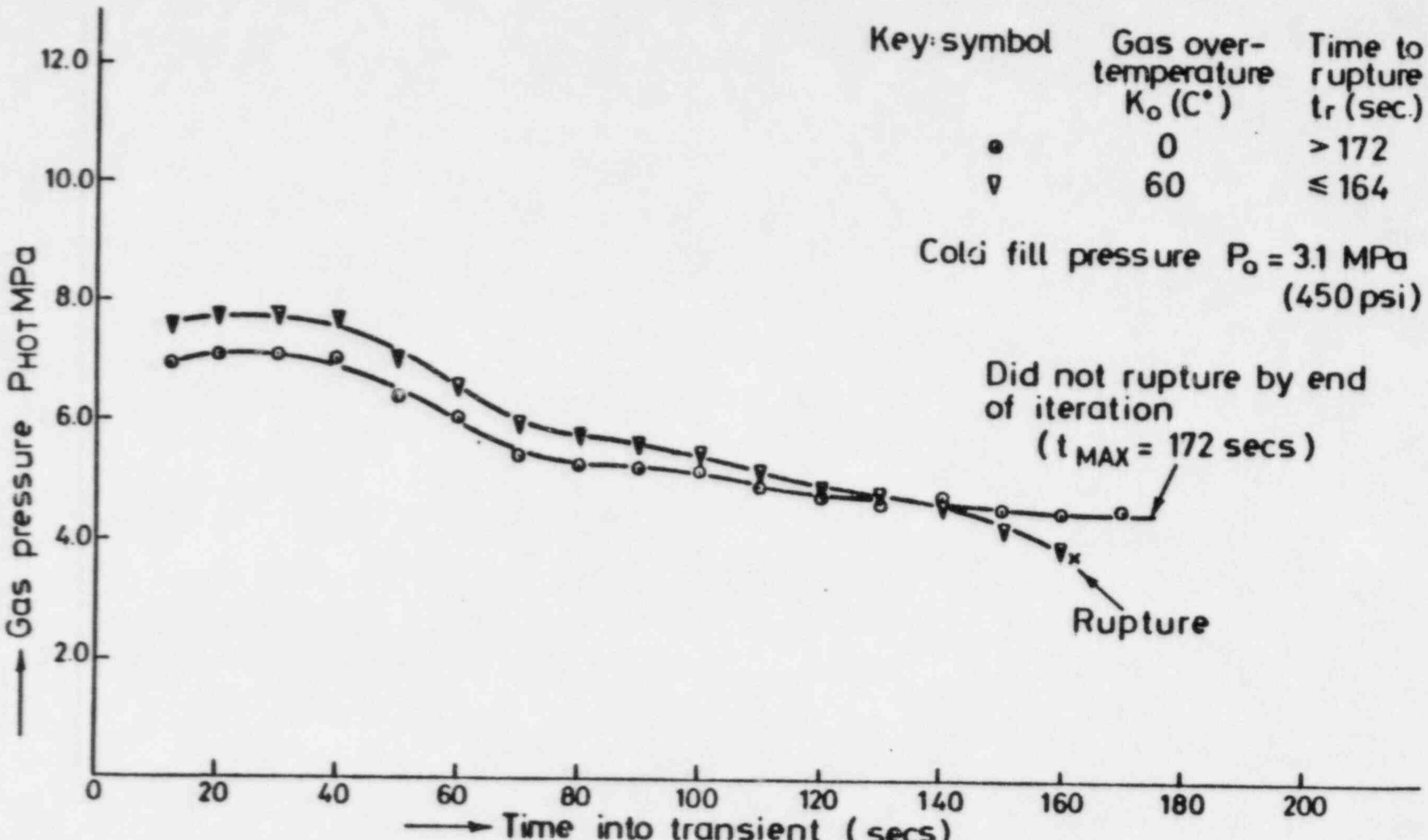

FIG.5a. Variation of Internal Gas Pressure, P_{HOT}, with Time during a Ballooning Transient for an Initial Cold Fill Pressure, P_o, of 3.1 MPa.

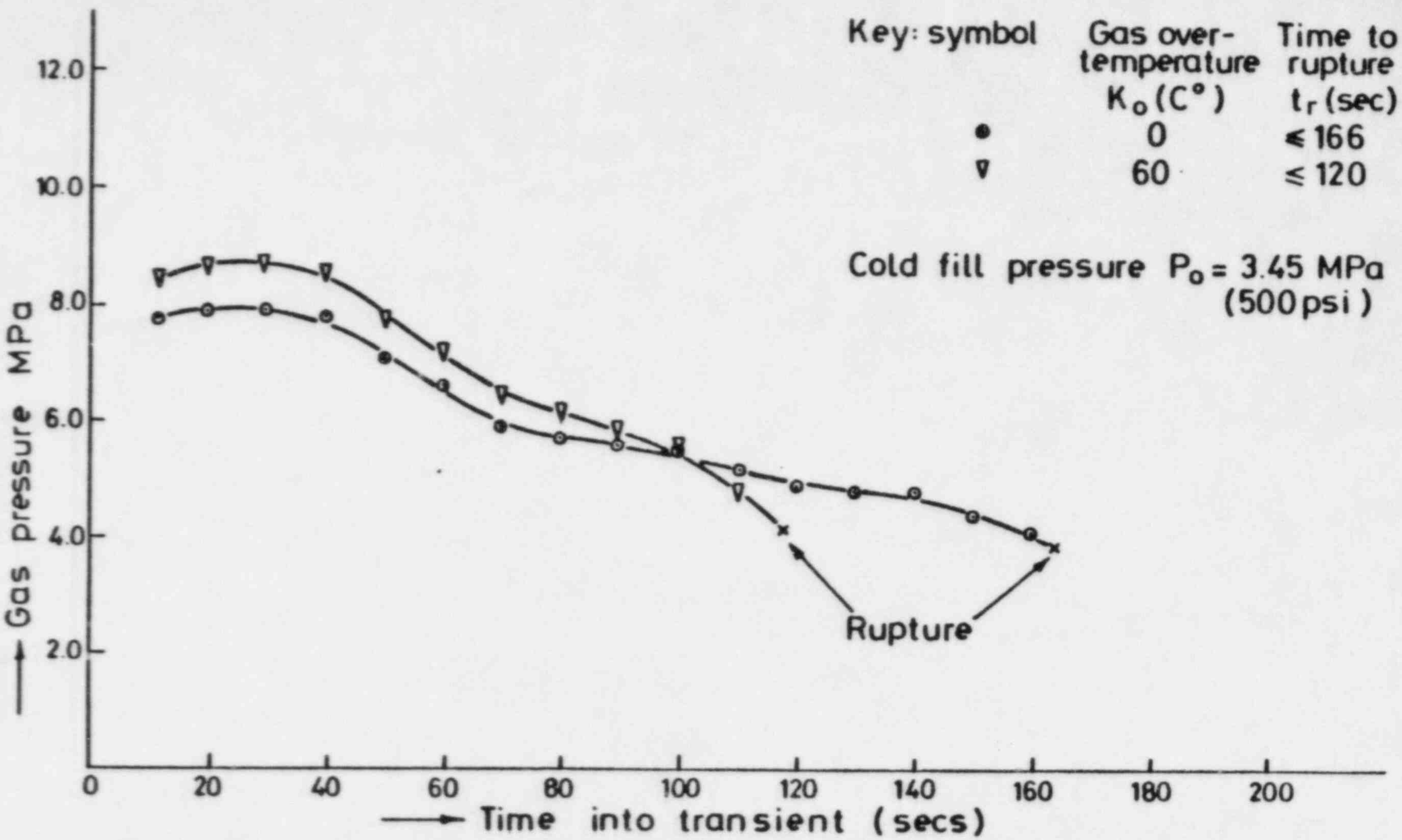

FIG. 5b. Variation of Internal Gas Pressure, P_{HOT}, with Time during a Ballooning Transient for an Initial Cold Fill Pressure P_o of 3.45 MPa.

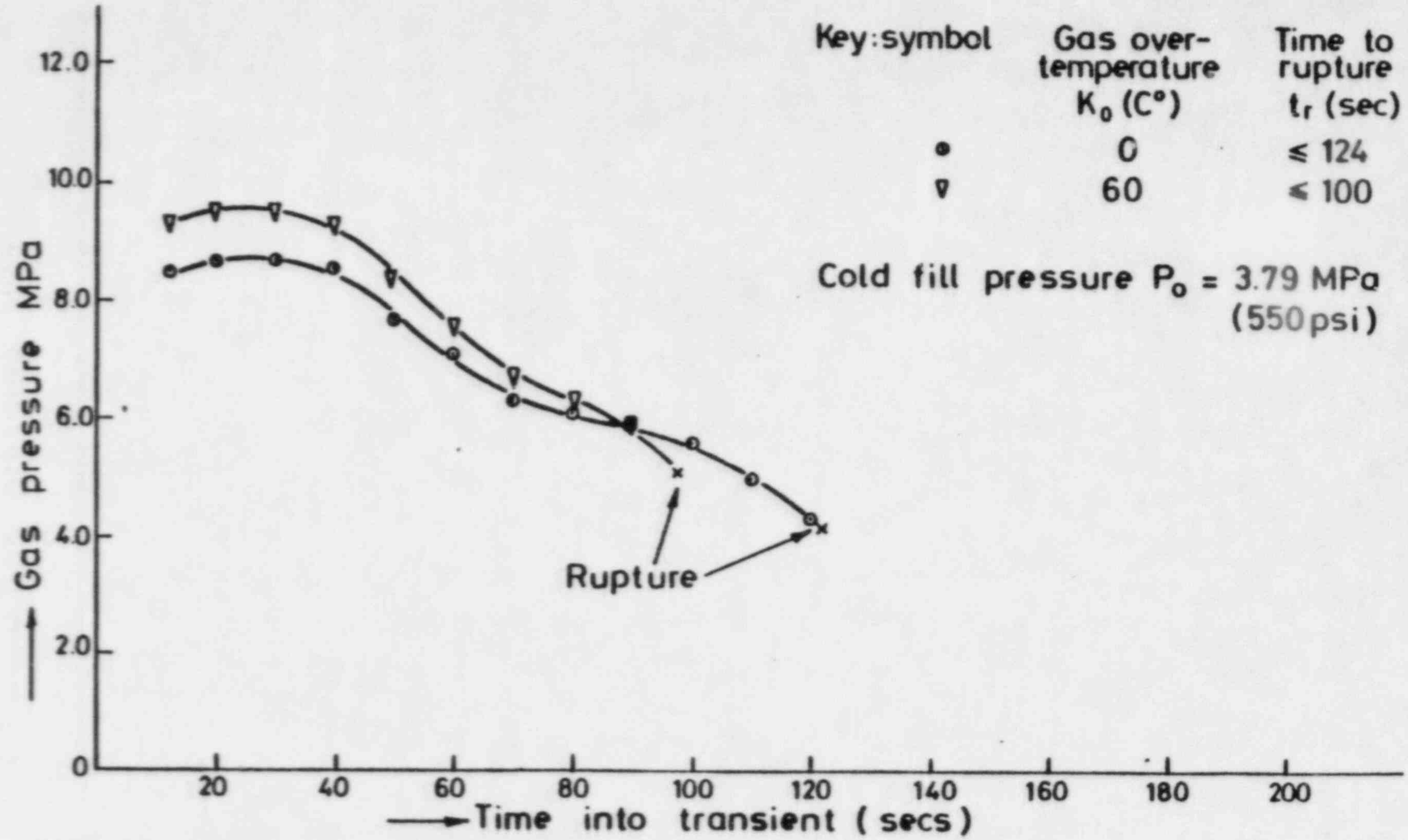

FIG. 5c. Variation of Internal Gas Pressure, P_{HOT}, with Time during a Ballooning Transient for an Initial Cold Fill Pressure, P_o, of 3.79 MPa.

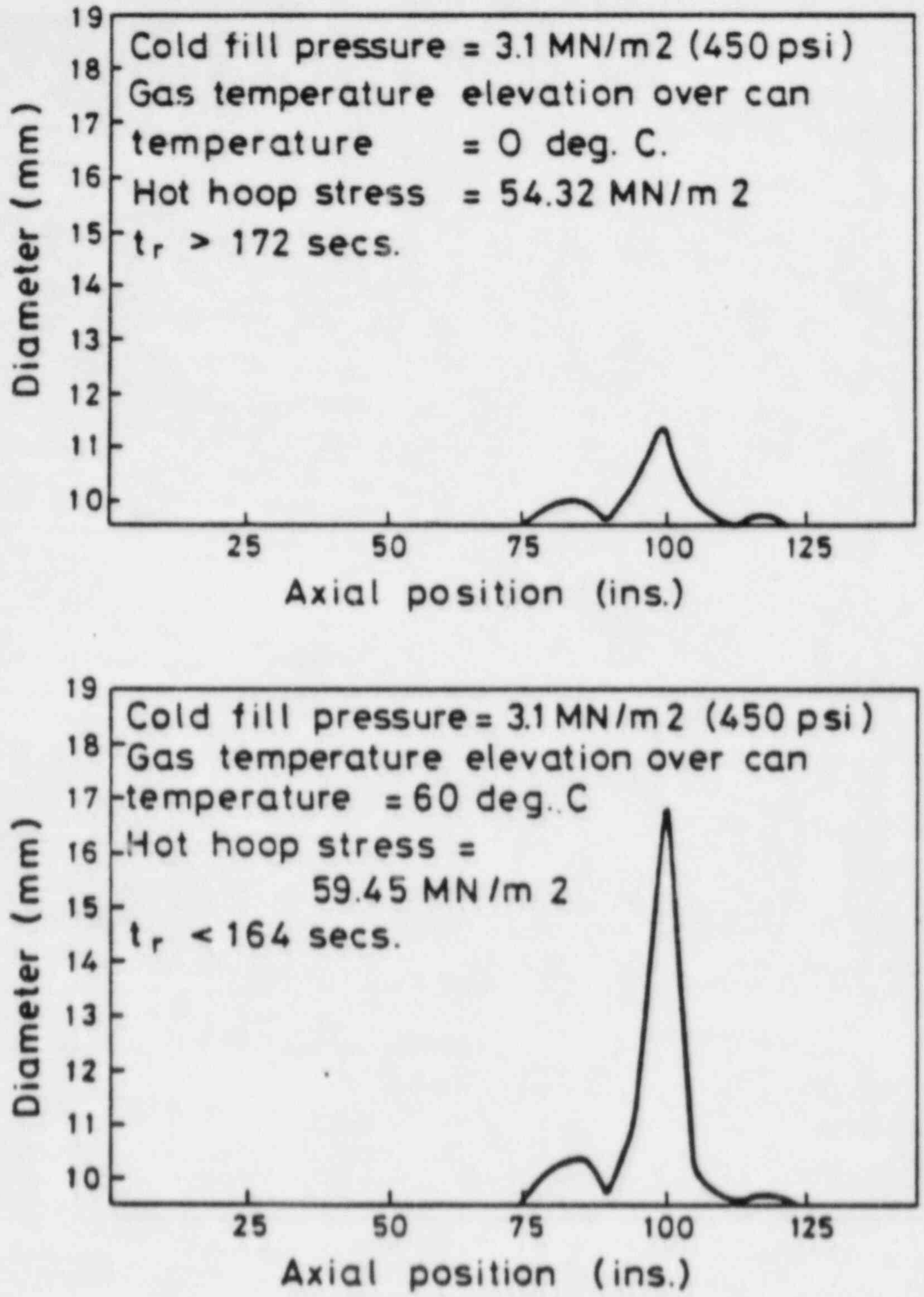

FIG. 6. Variation of Calculated Rod Diameter as a Function of Axial Location.
(Thermal History as in Table 2.)

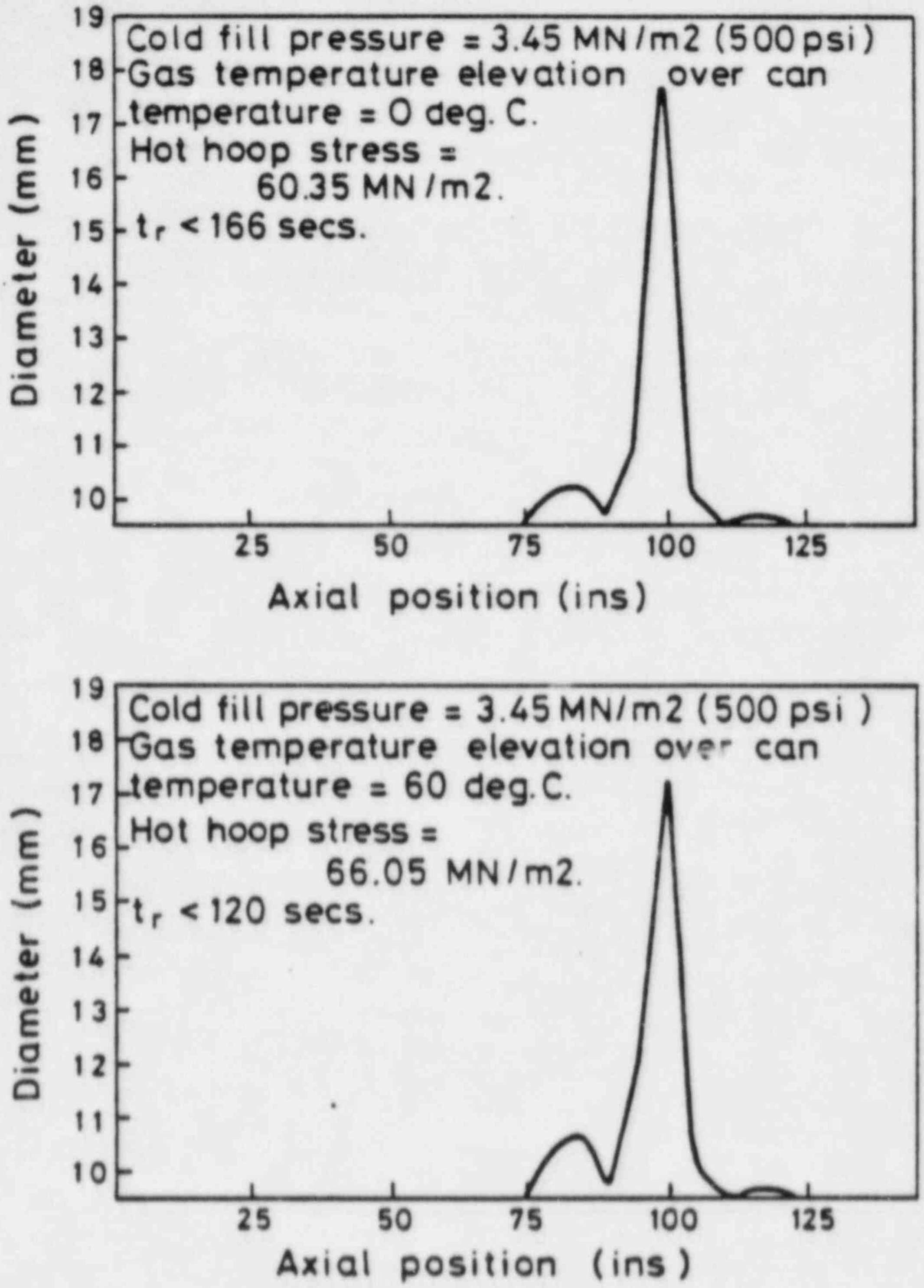

FIG. 7. Variation of Calculated Rod Diameter as a Function of Axial Location.
(Thermal History as in Table 2.).

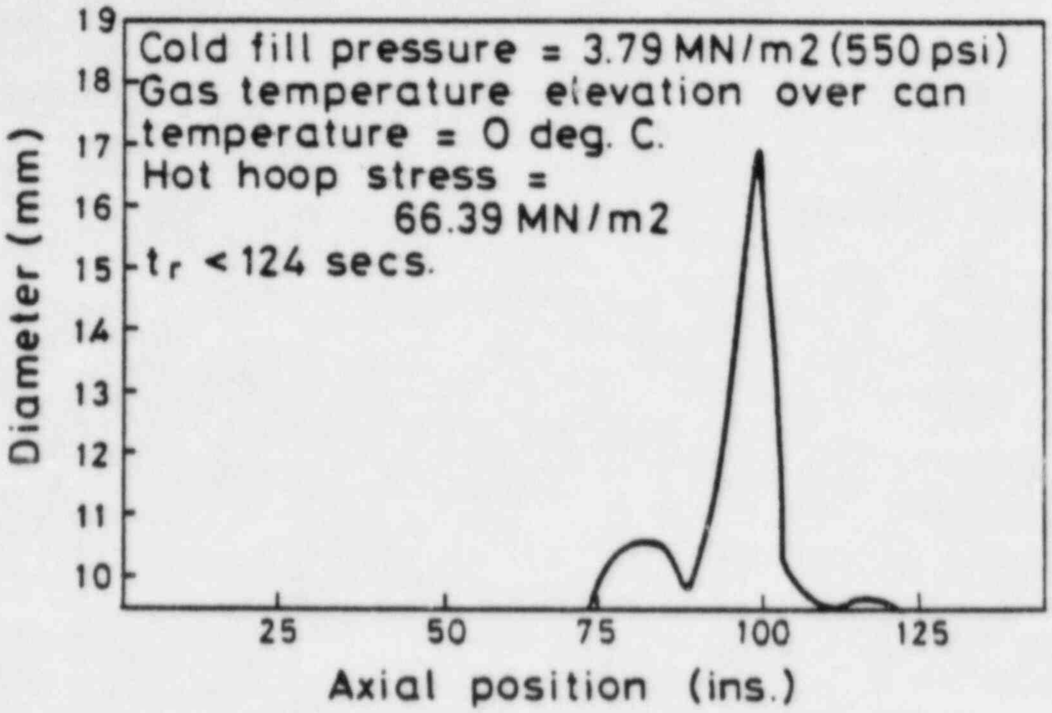

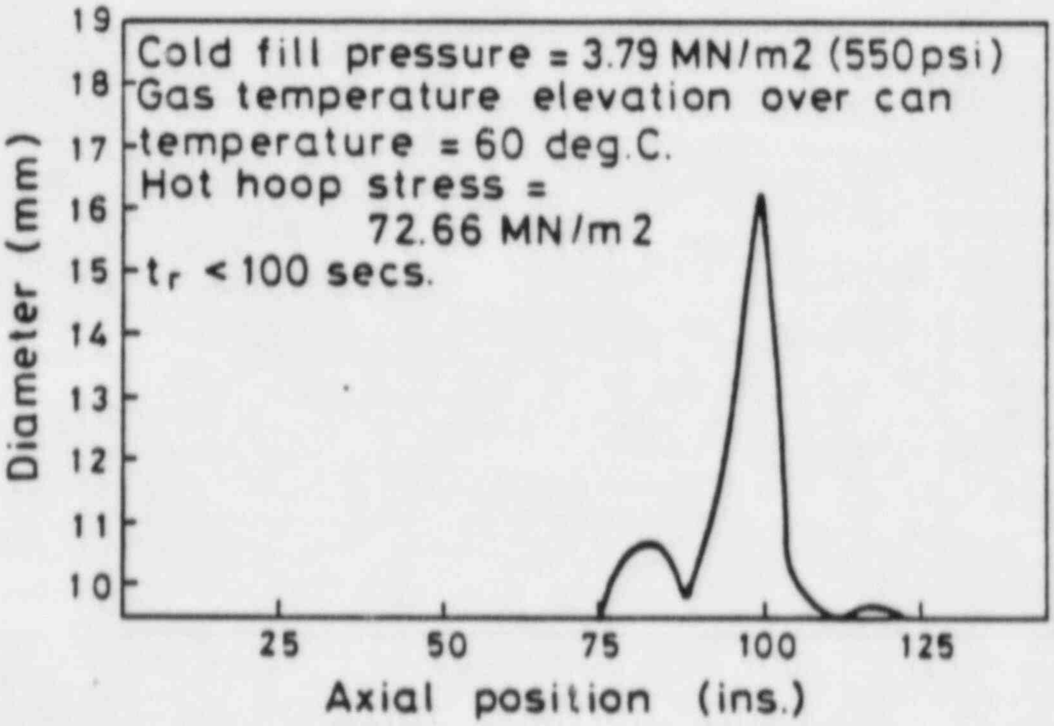

FIG.8. Variation of Calculated Rod Diameter as a Function of Axial Location.
(Thermal History as in Table 2.).

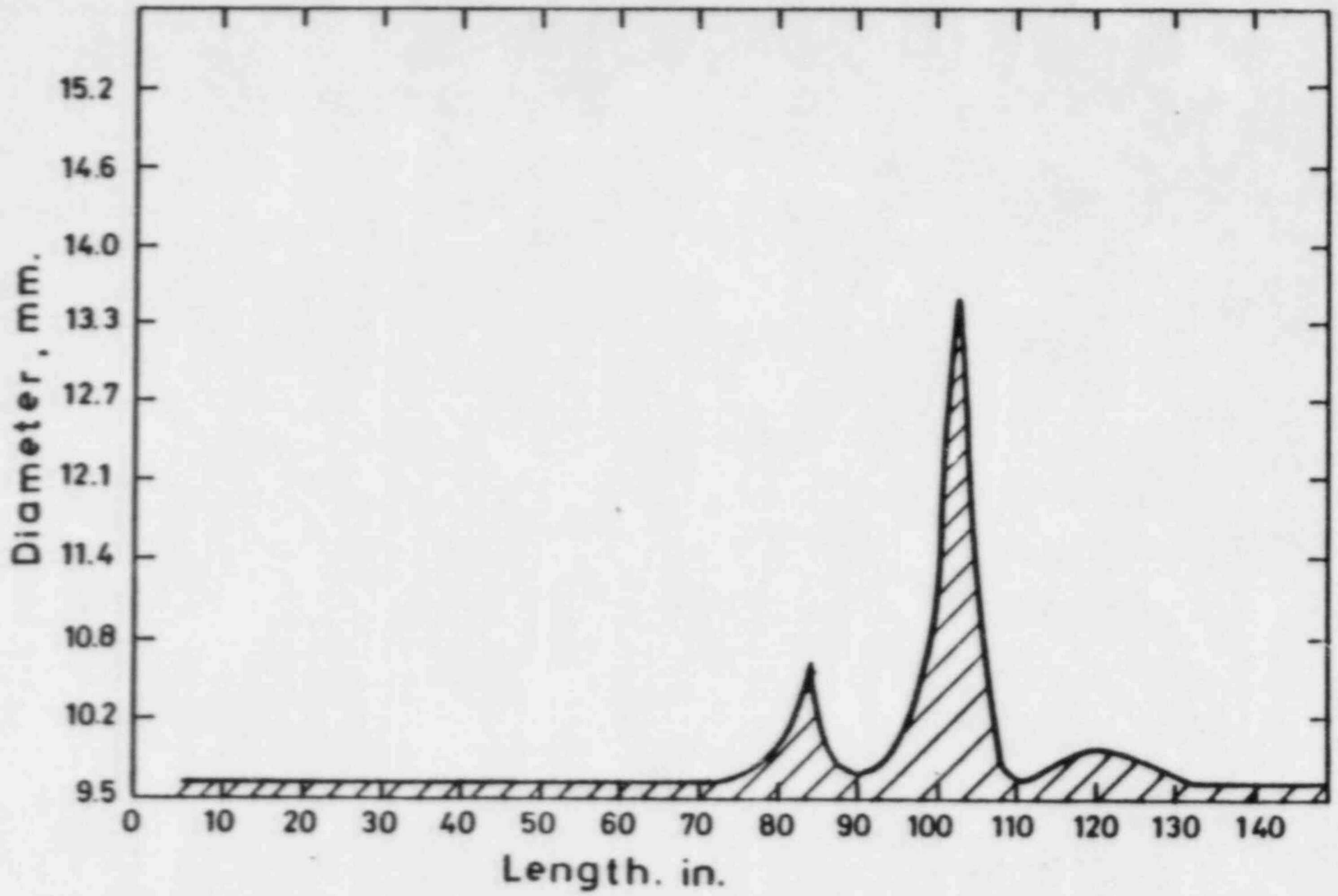

FIG. 9. Average Diametral Measurement versus Axial Elevation for a Typical Fuel Rod in Test MT-3.

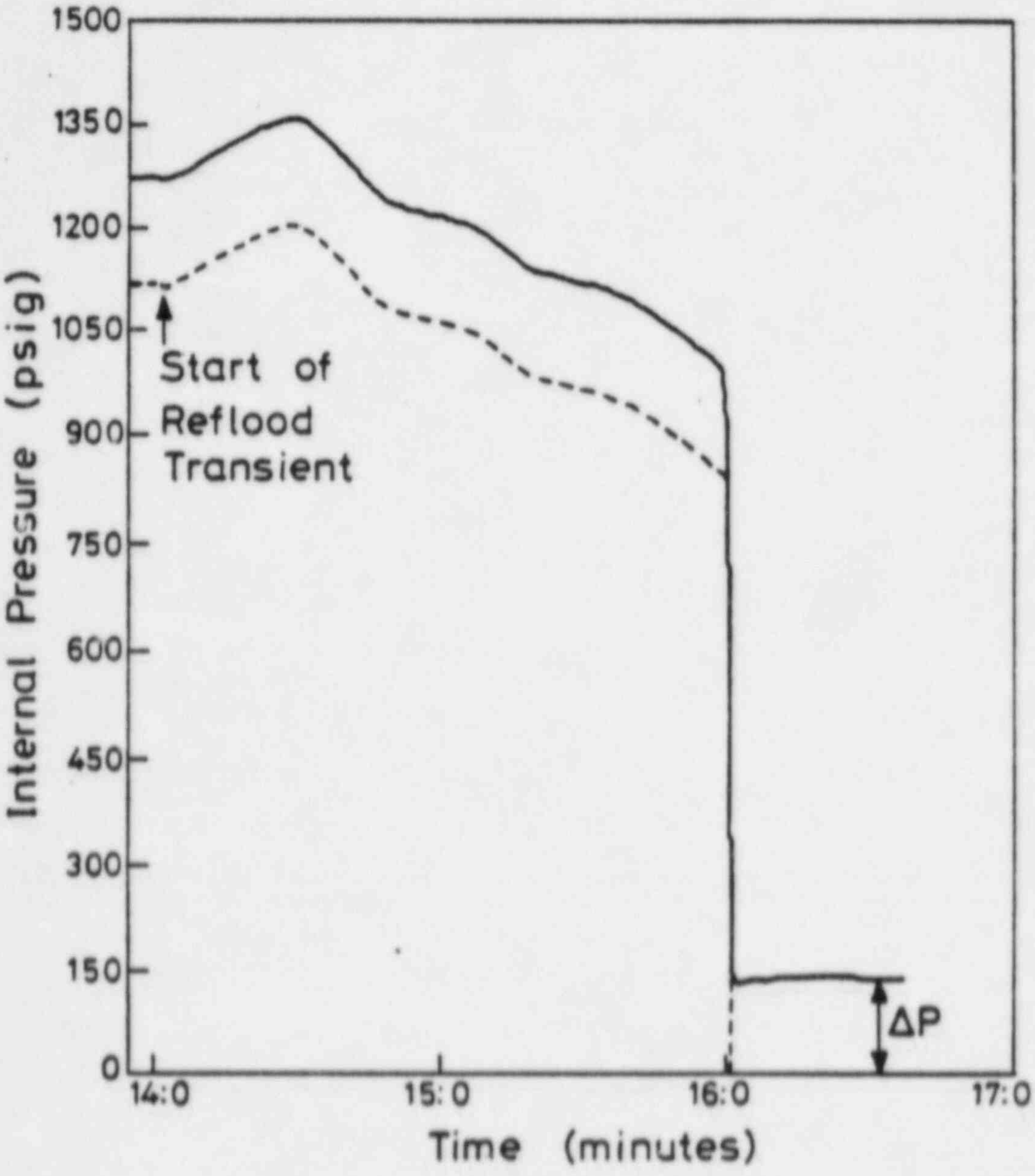

FIG. 10. Measured Variation of the Internal Pressure of Rod During Ballooning

DISTRIBUTION

TPRD/B/0101/N82

S	Dr T Broom		
S	Director		Berkeley Nuclear Laboratories
S	Dr P F Chester		
S	Dr E W Carpenter		
S	Dr D J Silverleaf		Headquarters
S	Dr J K Wright		"
S	Dr D A Dominey		SE Region
S	Mr M E Peplow		SW Region
S	Mr H F J Hadrill		Midlands Region
S	Mr H G Masterson		NE Region
	Dr D E Jeffers		NW Region
S	Mr P M Billam		Generation Development & Construction Div.
S	Mr B V George		"
S	Dr B Edmondson		Nuclear Ops Support Group
S	Mr R L Rutter		"
S	Dr R S Hall		Berkeley Nuclear Laboratories
	Dr B C Masters		"
S	Dr J E Antill		"
S	Mr C H A Townley		"
S	Dr K E G Meredith		"
	Dr K H Jolliffe		Central Electricity Research Laboratories
S	Mr L P Chadwick		Marchwood Engineering Laboratories
S	Mr J C Metcalfe		"
S	Dr S Blow		Headquarters
S	Mr F Broomhead		"
	Reports Librarian	(3)	"
	Librarian		Berkeley Nuclear Laboratories
	Librarian		Central Electricity Research Laboratories
	Librarian		Marchwood Engineering Laboratories
	Librarian		SSD Midlands Region
	Librarian		SSD SE Region
	Mr D E Wetherly		" (Bankside)
	Librarian		SSD NE Region
	Librarian		SSD NW Region
	Librarian		SSD SW Region
	Technical Serv. Manager		SSEB, East Kilbride
	Librarian		SSEB
	Librarian		UKAEA, Risley
	Librarian		AECL, Chalk River, Canada
S	Librarian		AECL, Whiteshell, Canada
	Librarian		CEN, Saclay, France
	Librarian		Centro Informazioni Studi Esperienze, Italy
	Librarian		Euratom, Brussels
	Librarian		Studsvik Energiteknik AB, Sweden
	Librarian		ECN, Petten, Netherlands
	Mr R Rudman	(2)	EPRI, California, USA
	Mr F J Simpson		Ontario Hydro, Canada
	Ms S S Ray		TVA, Chattanooga, USA
	Dr P M Kelly		AAEC, Lucas Heights
	Mr E Goldfinch		NTP, Ashford, Kent
	Mr D S L Danford		Headquarters (China NPIC)

Mr R R Matthews	Health and Safety Department
Librarian	UKAEA, Harwell
Librarian	UKAEA, Springfields
Librarian	UKAEA, Windscale
Librarian	UKAEA, Winfrith
Dr M L Picklesimer	USNRC, Washington, USA
Dr D Powers	"
Mr R Van Houten	"
Dr G Marino	"
Dr M Silberberg	"
Dr R O Meyer	"
Dr R B Duffey	EPRI, California
Mr C E Ells	AECL, Chalk River, Canda
Dr M Nottley	"
Mr D Nishimura	"
Dr L Hunt	"
Dr H E Sills	"
Dr H Rosinger	AECL, Whiteshell, Canada
Dr M G Wright	"
Dr F Wunderlich	Kraftwerk Union, Erlangen, Germany
Dr G Cheliotis	"
Dr A Fiege	Karlsruhe GFK, Germany
Dr F Erbacher	"
Dr K Weiss	"
Dr S Leistikow	"
Dr M Bocek	"
Dr S Raff	"
Dr T F Kassner	Argonne National Laboratory, Illinois, USA
Dr R H Chapman	Oak Ridge National Lab., Tennessee, USA
Mr D L Burman	Westinghouse, Pittsburgh, USA
Mr L Hochreiter	"
Dr A L Lowe	Babcock and Wilcox
Dr C Mohr	Battelle-Pacific Northwest Laboratories, Richland, Washington, USA
Mr J Pilger	"
Mr G Hesson	ISPRA, Varese, Italy
Dr H Ohno	Central Research Institute of the Electric Power Industry, Iwato-Ikta, Komae-Shi, Tokio 182, Japan
Dr S Kawasaki	Japan Atomic Energy Research Institute, Tokai-Mura Naka-Gun, Ibaraki-Ken 319-11, Japan.
Dr M Ishikawa	"
Dr P MacDonald	EG & G Idaho National Eng. Lab., Idaho, USA
Dr J H Gittus	UKAEA Springfields
Mr J M Hartog	"
Mr C A Mann	"
Mr E D Hindle	"
Dr C Bilsby	"
Mr J B Sayers	AERE Harwell
Mr D J Clough	"
Mr D A Banks	UKAEA Windscale
Mr A Garlick	"
S Dr V W Eldred	"

Dr D Hicks		UKAEA Risley
Mr J Stephenson		"
Dr I H Gibson		UKAEA Winfrith
Dr P Coddington		"
Mr J Fell		"
Mr K G Pearson		"
Mr R Bowring		"
Mr L Raven		BNFL Springfields
Dr C C Baylis		"
Mr D Howl		"
Mr J A Scott		NNC Whetstone
Mr J N Baker		"
Mr D A Ward		"
Mr T C Beswick		CEGB, Barnwood
Mr C R Simons		"
Mr W J Kilgour		"
Mr A Oastler		"
Mr M J Arnold		CEGB HSD Courtenay House
Mr A C Willetts		"
Mr J R Harrison		"
Mr R A Bruce		Westinghouse C/O NNC Whetstone
Mr L G Williams		NII Thames House
Dr J S Waddington		Berkeley Nuclear Laboratories
Mr M V Speight		"
Dr T Healey		"
Dr A T Donaldson	(5)	"
Mr A F Brown		"
Dr H E Evans		"
Dr G Knowles		"
Dr R C Lobb		"
Dr B Burton		"
Dr G L Reynolds		"
Dr G Roberts		"
Mr R A L Horwood		"
Dr S J Board		"
Mr K Ardron		"
Mr S Fairbairn		"

REPORT SUMMARY SHEET

Central Electricity Generating Board

Berkeley Nuclear Laboratories

CEGB UNCLASSIFIED

TPRD/B/0101/N82
WR/FBWG/P(82)68

Job No. XC176

Pre-Test Prediction and Post-Test Analysis of PWR Fuel Rod Ballooning in the MT-3 In-Pile LOCA Simulation Experiment in the NRU Reactor

by A.T. Donaldson, R.A. Horwood and T. Healey

For the attention of the Fuel Behaviour Working Group

JUNE 1982

SUMMARY

The USNRC and the UKAEA have jointly funded a series of in-pile LOCA simulation experiments in the Canadian NRU reactor in order to secure further information on the thermal hydraulic and clad deformation response of PWR fuel rod bundles. Test MT-3 in the series was performed using reflood rate and rod internal pressure conditions specified by the UK nuclear industry. The parameters were selected to ensure the development of a near-isothermal clad temperature history during which zircaloy was required to balloon and rupture near the alpha→alpha/beta phase transition. Specification of the reflood rate conditions was assisted by the performance of a precursor test on an unpressurised rod bundle and by complementary application of appropriate thermal hydraulic analyses. Identification of the rod internal pressure needed to cause ballooning and rupture was achieved using a creep deformation model, BALLOON, in conjunction with the clad thermal history defined by the prior thermal hydraulic test. This paper presents the basis of the BALLOON analysis and describes its application in calculating the fill gas pressure for rods MT-3, their axial ballooning profile and the clad temperature at peak radial strain elevations.

J.S. Waddington

Approved